

The fabrication and analysis of a PbS nanocrystal:C₆₀ bilayer hybrid photovoltaic system

D M N M Dissanayake¹, R A Hatton², T Lutz³, R J Curry⁴ and S R P Silva⁴

¹ Solid State Electronics Laboratory, University of Michigan, Ann Arbor, MI 48109-2122, USA

² Department of Chemistry, University of Warwick, Coventry CV4 7AL, UK

³ Department of Chemistry, Imperial College, London SW7 2AY, UK

⁴ Advanced Technology Institute, University of Surrey, Guildford GU2 7XH, UK

E-mail: ndissa@umich.edu


Received 8 March 2009, in final form 21 April 2009

Published 26 May 2009

Online at stacks.iop.org/Nano/20/245202

Abstract

A near-infrared sensitive hybrid photovoltaic system between PbS nanocrystals (PbS-NCs) and C₆₀ is demonstrated. Up to 0.44% power conversion efficiency is obtained under AM1.5G with a short circuit current density (J_{sc}) of 5 mA cm⁻² when the PbS-NC layer is treated in anhydrous methanol. The observed J_{sc} is found to be approximately one-third of the maximum expected from this hybrid configuration, indicating the potential for further optimization. Crucial for device operation, a smooth film of nanocrystals is seen to form on the hole transporting poly(3,4-ethylenedioxythiophene):poly(styrenesulfonate) (PEDOT:PSS) layer deposited on the transparent electrode, facilitated through an ionic interaction between nanocrystal capping ligands and the PEDOT:PSS. The formation of the open circuit voltage in this system is seen to be influenced by an interfacial dipole formed at the hole-extracting electrode, providing insights for further optimization.

 Supplementary data are available from stacks.iop.org/Nano/20/245202

1. Introduction

Organic photovoltaics (OPVs) have strong potential as a low cost method of electricity generation for the future. Up to 6% power conversion efficiency (η) has been demonstrated from OPVs based on polymer/C₆₀-derivative bulk heterojunctions and, furthermore, the scalability and stability of such systems is also well documented [1]. Inorganic semiconductor nanocrystals, possessing tunable optical bandgaps, can also be combined with organic semiconductors to fabricate hybrid photovoltaic devices with broad spectral sensitivity. To this end, hybrid photovoltaic devices with polymer or small molecule organic semiconductors used in combination with semiconductor nanocrystals (quantum dots and rods) have reported η up to 2.8% [2, 3]. The nanocrystals utilized in these reports were limited to wide bandgap Cd based chalcogenides that do not harvest near infrared photons ($\lambda > 750$ nm) which comprise $\sim 47\%$ of AM1.5G (1000 Wm⁻²) spectral

power density. Single layer infrared sensitive PbS nanocrystal (PbS-NC) Schottky type photovoltaic devices have recently demonstrated $\eta \sim 1.8\%$ [4]. Unfortunately, PbS-NCs/organic semiconductor hybrid photovoltaics which exhibit light harvesting in the near infrared have thus far yielded η values of less than 0.01% [5, 6]. In this paper we demonstrate a PbS-NC/fullerene based hybrid PV which exhibits up to 5 mA cm⁻² short circuit current density (J_{sc}) together with η of 0.44% under AM1.5G simulated solar irradiation measured in ambient conditions. A peak external quantum efficiency (EQE) of 35% at 400 nm and up to 5% EQE in the infrared region between 700 and 1100 nm is demonstrated. Furthermore, evidence for an interaction between the hole-extracting poly(3,4-ethylenedioxythiophene):poly(styrenesulfonate) (PEDOT:PSS) electrode and the PbS-NC capping surfactant groups is also reported, which is seen to facilitate smooth nanocrystal film formation. The open circuit voltage (V_{oc}) is found to be critically dependent on the nature of the

PbS-NC and the PEDOT:PSS interface, pointing the way to further device optimization.

2. Experimental details

Ligand capped quantum dots were synthesized according to a method reported elsewhere [7]. All chemicals were analytical reagent grade and were used as-received unless otherwise stated. Nine hundred milligrams of lead oxide (Sigma-Aldrich, 99.9%) was mixed with 1.6 g of oleic acid (Sigma-Aldrich, tech. 90%) and 40 ml of 1-octadecene (Fluka, $\geq 95\%$), and the mixture was heated to 130 °C under nitrogen and maintained at this temperature for 30 min. Twenty milliliters of a stock solution obtained by mixing 5 ml of hexamethyldisilthiane (Fluka) and 240 ml of 1-octadecene was then quickly injected into lead oleate precursor prepared earlier and kept at 70 °C for 20 min. The mixture was subsequently allowed to cool down and acetone was added to precipitate the PbS-NCs. After separation via centrifugation (8000 rpm for 5 min) and further washing with acetone, the PbS-NCs were suspended via ultrasonication in anhydrous chloroform and centrifuged at 5000 rpm for 5 min to remove aggregates. Prior to device fabrication the oleic acid ligands of PbS-NC were exchanged with shorter butylamine ligands. To perform ligand exchange [8], the dots were dried under nitrogen flux and then resuspended in an excess of butylamine (Fluka, 99.5%). After 72 h the PbS-NCs were precipitated out by addition of an excess of isopropanol and dissolved in chloroform. This operation was repeated several times for purification purposes. Subsequently the PbS-NCs were dissolved in toluene at a concentration of 70 mg ml⁻¹ for device fabrication. The approximate size of these PbS-NCs was calculated as ~ 3.8 nm by applying the absorption onset value to theoretical models documented elsewhere [9]. Optical absorption characterization of the active layers was performed using a Varian Cary 5000 UV-vis-IR spectrophotometer.

Photovoltaic devices were fabricated on 150 nm thick indium-tin oxide (ITO) ($20 \Omega/\square$) coated glass cleaned using a three-stage ultrasonic bath treatment in toluene, an aqueous surfactant solution and acetone. Immediately prior to use, the ITO substrates were subjected to oxygen plasma treatment for 5 min. PEDOT:PSS (Sigma-Aldrich) was spin coated onto ITO at 3000 rpm for 1 min prior to annealing in the ambient at 130 °C for 10 min. PbS-NC films were prepared on top of PEDOT:PSS coated ITO glass by spin casting at 2000 rpm from a 70 mg ml⁻¹ toluene solution. The thickness of the resulting PbS-NC layer was measured to be 100 nm by a Dimension 3100 atomic force microscope (AFM). Afterwards, the PbS-NC coated substrates were immersed in anhydrous methanol for approximately 10 s to remove capping surfactants. It was shown by Konstantatos *et al* that PbS-NC films soaked in methanol for 2 h caused a decrease in the interparticle separation, resulting in a remarkable increase of the dark current density [8]. A similar approach was used in our experiments to remove the butylamine ligands but much shorter timescales were used (< 10 s). A longer soaking time (several minutes) resulted in increased desorption of the nanocrystals from the PEDOT:PSS, reducing

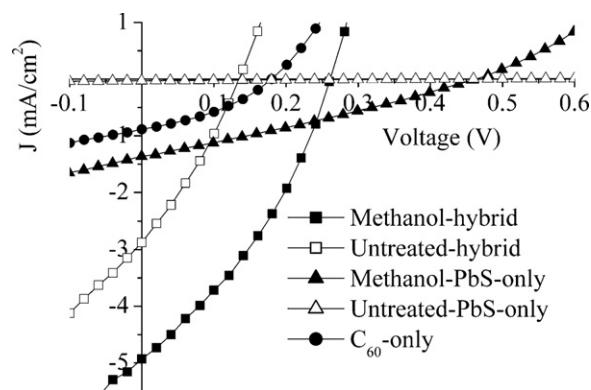


Figure 1. Current density–voltage characteristics of ITO/PEDOT:PSS/PbS-NC/C₆₀/BCP/Al photovoltaic devices treated in methanol for 10 s (dark squares) and untreated (white squares). The current density–voltage characteristics of ITO/PEDOT:PSS/C₆₀/BCP/Al (C₆₀-only) (dark circles) and ITO/PEDOT:PSS/PbS-NC/BCP/Al (PbS-only) photovoltaic devices treated in methanol for 10 s (dark triangles) and untreated (white triangles) are also given. All photovoltaic devices were measured under AM1.5G simulated solar irradiation.

the device performance. Therefore, an optimum soaking time was obtained empirically using a series of photovoltaic devices fabricated after washing in methanol for different time periods, ranging from 10 s up to 10 min, and it was observed that optimum device characteristics were obtained for shorter soaking times (supplementary figure S1 available at stacks.iop.org/Nano/20/245202). Discrete heterojunction photovoltaic devices were fabricated by the subsequent vapour deposition of a 30 nm film of C₆₀ at $\sim 10^{-5}$ Torr at a deposition rate of ~ 0.1 nm s⁻¹. A 10 nm layer of bathocuproine (BCP) (Sigma-Aldrich) was evaporated onto the C₆₀ layer at a deposition rate of ~ 0.1 nm s⁻¹ followed by deposition of an aluminium top electrode using a shadow mask to create active device areas of ~ 10 mm² which were defined by 2×5 mm² rectangles. *JV* characteristics were obtained using a Keithley 2400 source meter under AM1.5G simulated solar irradiation obtained from an Oriel 81160 class B solar simulator with $\leq 5\%$ non-uniformity of irradiance. EQE measurements were made using a Bentham IL1 100 W quartz halogen light source, a Bentham TMc 300 monochromator, a Keithley 487 picoammeter, a Newport 1830C optical power meter, and 818-SL and 818-IG photodetectors. Both *JV* and EQE measurements were carried out in ambient conditions. Approximate lifetimes of the devices were observed to be less than 20 min in ambient conditions. Kelvin probe measurements were performed under a nitrogen atmosphere. Changes in work function were measured with respect to the contact potential difference between the oscillating probe and freshly prepared PEDOT:PSS coated ITO glass substrate.

3. Results and discussion

Figure 1 shows a comparison of the current density/voltage (*JV*) characteristics of PbS-NC/C₆₀ (hybrid) photovoltaic with C₆₀ and PbS-NC single layer reference devices. The hybrid and PbS-only reference devices were fabricated with

and without soaking in methanol (approximately 10 s). The methanol treated hybrid photovoltaic device (methanol-hybrid) demonstrates the largest J_{sc} (5 mA cm^{-2}) and highest η (0.44%). Soaking in methanol clearly increases the J_{sc} of the methanol-hybrid (5 mA cm^{-2}) and PbS-NC single layer device (1.4 mA cm^{-2}) as compared to untreated device equivalents which demonstrated 3.0 mA cm^{-2} and 0.03 mA cm^{-2} , respectively. The increase in J_{sc} is attributed to enhanced carrier mobility within the nanocrystal film attributed to increased inter-dot coupling as a result of the removal of the capping butylamine ligands [8]. The relative increase in J_{sc} of the single layer PbS-NCs photovoltaic devices upon methanol treatment (45-fold) is far greater than the J_{sc} increase (less than two-fold) of the hybrids. This can be explained by the different exciton dissociation and charge transport mechanisms found in the two device architectures: in single layer PbS-NC photovoltaic devices the exciton dissociation occurs at the electrode interfaces and therefore J_{sc} depends solely on charge flow through the PbS-NC film. As a result, the change in carrier mobility of the nanocrystal has a direct impact on J_{sc} , as seen. Conversely, exciton dissociation in the hybrid devices occurs at the heterojunction and J_{sc} depends on carrier transport through both PbS-NC and C_{60} phases. Therefore it is reasonable to expect less change of J_{sc} with changes to the carrier mobility of the nanocrystal film, rationalizing the above observations. Hybrid systems, treated or not, show larger J_{sc} compared to the C_{60} -only reference (0.88 mA cm^{-2}), indicating increased photocurrent generation from the nanocrystals together with enhanced exciton dissociation at the heterojunction.

EQE measurements were carried out to measure the light harvesting capability of the nanocrystals within the hybrid system. As shown in figure 2, at 400 nm the methanol-hybrid device exhibits up to 34% EQE as compared to 15% EQE shown by the C_{60} -only reference. Furthermore, the methanol-hybrid device exhibits two orders of magnitude greater EQE ($\sim 5\%$) in the near infrared compared to the C_{60} -only reference device, explaining the larger J_{sc} . Also, by comparing the J_{sc} of the methanol-PbS-only device (1.4 mA cm^{-2}) to the methanol-hybrid device (5 mA cm^{-2}) it can be seen that a larger photocurrent can be in principle obtained from a donor-acceptor type as opposed to single layer Schottky type architecture.

As seen in figure 1, the V_{oc} of the hybrid photovoltaic device is observed to increase from 0.13 V for the untreated hybrid to 0.26 V for the methanol treated hybrid device. It is generally accepted that the maximum attainable V_{oc} in OPVs is given by the difference between the lowest unoccupied molecular orbital (LUMO) energy of the acceptor and the highest occupied molecular orbital energy (HOMO) of the donor [10]. However, there is less consensus as to the extent to which the work function of the electrodes plays a role in determining V_{oc} [11, 12]. Based on measurements of the ionization potential of PbS-NCs (5.2 eV) [13] and the electron affinity of C_{60} (4.5 eV) [14] the maximum attainable V_{oc} in the PbS-NC/ C_{60} hybrid system described herein is 0.7 eV. However, it is clear from figure 1 that V_{oc} falls well short of 0.7 V in hybrid devices with and without methanol treatment, which indicates that the work function of the hole-extraction

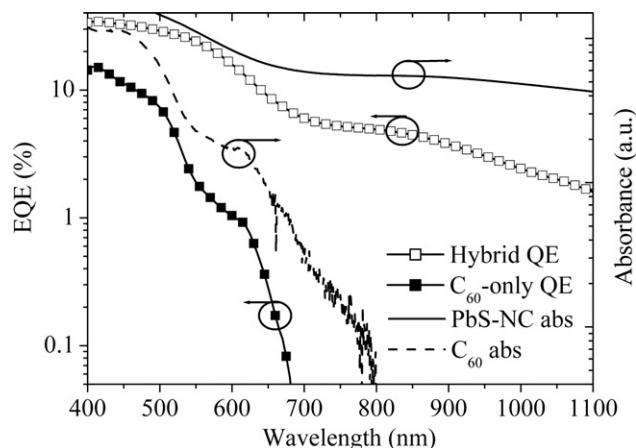


Figure 2. External quantum efficiency of a ITO/PEDOT:PSS/PbS-NC/ C_{60} /BCP/Al device treated in methanol for 10 s (methanol-hybrid), shown by the white squares line. The external quantum efficiency of a ITO/PEDOT:PSS/ C_{60} /BCP/Al (C_{60} -only) device is shown by the dark squares line. The absorbance of PbS-NC and C_{60} films deposited on quartz are shown by a solid line and dashed line, respectively.

electrode plays a role in determining V_{oc} in devices of this type. Since the Fermi level of aluminium is reportedly pinned to the LUMO of C_{60} (4.5 eV) [11] and the work function of PEDOT:PSS is $\sim 5.1 \text{ eV}$ [15] the absolute anode-cathode energy difference is $\sim 0.6 \text{ eV}$. However, the V_{oc} achieved is at least a factor of two smaller than 0.6 V. To explain this result we propose the formation of an interfacial dipolar layer at the PEDOT:PSS/PbS-NC heterojunction which acts to reduce the work function of the PEDOT:PSS contact, thereby reducing the V_{oc} . The formation of interfacial dipoles resulting in negative interfacial vacuum level shifts as large as 1 eV is well known to occur at many metal-organic interfaces, not always as the result of a chemical interaction [16]. In the current context the electropositive nature of butylamine ligands may act to reduce the PEDOT:PSS work function in one of two ways. (i) The surface of PEDOT:PSS is known to be PSS rich [15] and so it is possible that the sulfonic acid groups interact chemically with the weakly bound amine ligands via an acid-base type interaction, resulting in the formation of an interfacial dipole pointing away from the electrode surface. (ii) Alternatively, it is possible that a dipole is induced in the weakly polar, but electron rich, alkylamine ligand because of its close proximity to the intrinsically polar PEDOT:PSS surface. From figure 1 it is seen that when the PbS-NC layer is washed with methanol to remove the butylamine ligands the hybrid photovoltaic devices show increased V_{oc} . It is likely that washing with methanol at least partially removes the butylamine ligand at the buried interface and improves the contact with PEDOT:PSS by partial dissolution or softening of the PEDOT:PSS surface, since PEDOT:PSS is known to be soluble in alcohols. To test this hypothesis we used a Kelvin probe to measure the change in the work function of PEDOT:PSS films on ITO coated glass upon brief exposure to *n*-butylamine, followed by rinsing in methanol for 10 s. The Kelvin probe method measures the spatial average contact potential difference beneath the probe and is ideally suited to measuring relative changes in work

function [17, 18]. Upon exposure to liquid *n*-butylamine—deposited by spin casting and drying in vacuum—the work function of PEDOT:PSS films decreased by ~ 0.42 eV. Upon subsequent rinsing in methanol for 10 s the work function then increased by ~ 0.27 eV. These results support the conclusion that the V_{oc} in these devices is a function of the work function of the hole-extracting electrode and are entirely consistent with the explanation given above based on the hypothesis of an interfacial dipole layer. Consequently, we believe that the path to achieving larger V_{oc} in these device structures is to minimize adverse interfacial dipole formation and increase the work function of the hole-extracting electrode to improve matching of the electrode Fermi level with the valence band of PbS-NCs. Further to the J_{sc} and V_{oc} properties discussed above, relatively small improvement of the fill factor (FF) from 0.3 to 0.35 is seen for the hybrid photovoltaic devices after treatment with methanol which also is attributed to the increase in the carrier mobility, resulting in nanocrystal films upon removal of the insulating capping ligands.

A study of the roughness of PbS-butylamine films spin coated onto bare ITO glass (figure 3(a)) and PEDOT:PSS coated ITO glass (figure 3(b)) using an AFM provided evidence for an attractive interaction between butylamine capped PbS-NCs (PbS-butylamine) and PEDOT:PSS. For comparison, as-synthesized oleic ligand capped PbS-NCs (PbS-oleic) were spin coated on bare ITO (figure 3(c)) and PEDOT:PSS coated ITO (figure 3(d)). The PbS-butylamine and PbS-oleic deposited on ITO glass exhibit comparable root mean square (rms) roughness (peak-to-peak height) of 10.84 nm (32.19 nm) and 10.18 nm (49.04 nm), respectively. PbS-oleic deposited on PEDOT:PSS (figure 3(d)) shows a similar roughness (10.65 nm) and comparatively similar average height (34.64 nm) to PbS-oleic on ITO (figure 3(c)). However, the PbS-butylamine deposited PEDOT:PSS sample (figure 3(b)) shows a large reduction in the roughness (average height); 2.84 nm (10.36 nm) as compared to that on the film on bare ITO (figure 3(a)). This remarkable reduction in roughness and average height cannot be attributed to the smoother nature of pristine PEDOT:PSS (rms 1.20 nm figure 3(f)) relative to the bare ITO substrates (rms 2.3 nm figure 3(e)).

This dramatic improvement in film forming properties is compelling evidence of an attractive interaction between the butylamine capped PbS-NCs and the PEDOT:PSS, since the extent to which the butylamine capped PbS-NCs wets the PEDOT:PSS surface is greatly improved. It is plausible that the sulfonic acid functionality at the PEDOT:PSS surface is responsible for the attractive interaction, possibly via displacement of the butylamine ligands attached to PbS-NCs or direct interaction with the electropositive butylamine ligands. Improved wetting of the substrate electrode by PbS-NC results in uniform film formation and superior device performance: photovoltaic devices fabricated on bare ITO glass were found to short circuit, correlating with the high roughness of the nanocrystal film and highlighting the importance of an attractive interaction between the nanocrystals and supporting substrate during the deposition process. This crucial aspect of smooth nanocrystal film formation for photovoltaic devices has been discussed in recent reports in the literature [4, 19, 20].

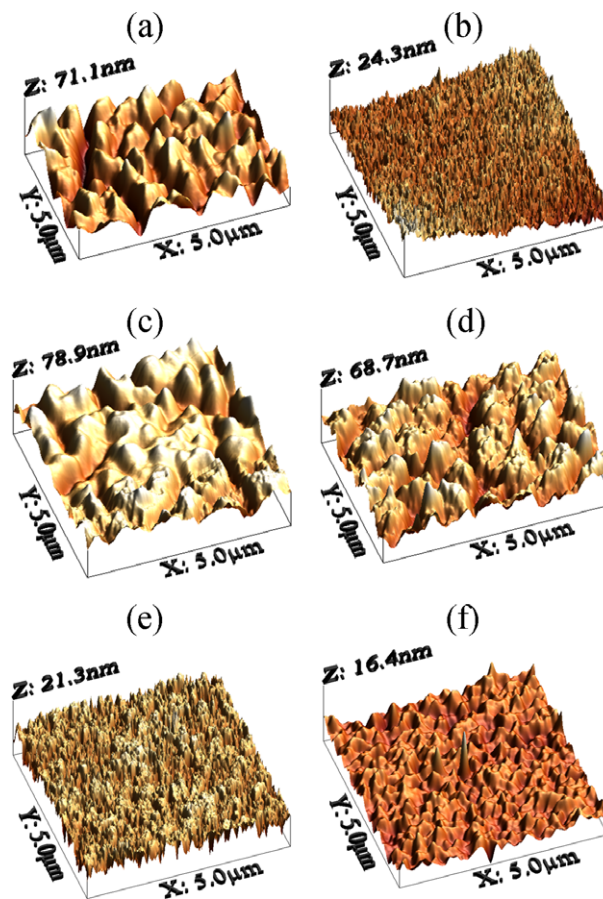


Figure 3. AFM images of butylamine ligand capped PbS-NCs deposited on (a) ITO and (b) PEDOT:PSS coated ITO, and oleic ligand capped PbS-NCs deposited on (c) ITO and (d) PEDOT:PSS coated ITO. Parts (e) and (f) show the AFM images of pristine ITO and PEDOT:PSS coated ITO, respectively.

(This figure is in colour only in the electronic version)

In order to increase the η of methanol treated hybrid devices the J_{sc} , V_{oc} and FF need to be increased further. A simplified model (supplementary figure S2 available at stacks.iop.org/Nano/20/245202) was utilized to estimate the maximum J_{sc} expected for a PbS-NC (100 nm) and C₆₀ (30 nm) bilayer hybrid PV device employing ITO and aluminium electrodes. The theoretical maximum J_{sc} was calculated using the quantum efficiency (η_{QE}) obtained as the product of absorption (η_{EA}), exciton diffusion (η_{ED}) and carrier collection (η_{CC}) efficiencies. For simplification, the η_{CC} was taken as unity. To obtain the maximum η_{ED} , the exciton diffusion length (1000 nm) of PbS-NCs was assumed to be larger than the PbS-NC layer thickness (100 nm). One hundred per cent and 0% reflection of light was assumed at the aluminium and ITO contacts, respectively. The exciton diffusion length of C₆₀ was obtained from the literature as (40 nm) [21] and the absorption coefficients for each material were determined from UV-vis-IR absorption measurements on samples with known thicknesses (supplementary figure S3 available at stacks.iop.org/Nano/20/245202). Using the AM1.5G solar spectrum between 400 and 1100 nm, the theoretical maximum

J_{sc} was obtained as 16 mA cm^{-2} , as seen in supplementary figure S4 (available at stacks.iop.org/Nano/20/245202). The J_{sc} obtained from the measured EQE (figure 2) over the same range of wavelengths was calculated to be 4.8 mA cm^{-2} , which is in good agreement with the measured J_{sc} value of 5 mA cm^{-2} shown in figure 1. Therefore, the methanol-hybrid device demonstrates approximately one-third of the maximum possible J_{sc} . This result shows that the efficiency with which photogenerated charge carriers are extracted to the external circuit must be improved to obtain greater J_{sc} values close to the theoretical maximum.

4. Conclusion

A near-infrared sensitive PbS-NC/C₆₀ hybrid photovoltaic device was fabricated and characterized. η values of up to 0.44% were obtained under AM1.5G simulated solar irradiation together with a J_{sc} of 5 mA cm^{-2} when the PbS-NC layer was soaked in anhydrous methanol for a short period. The improvement in device performance was attributed to increased carrier mobility of the PbS-NC film. The obtained J_{sc} was calculated to be approximately one-third of the maximum J_{sc} expected from the maximum bilayer hybrid photovoltaic experimentally demonstrated in this study. Smooth PbS-NC film formation on PEDOT:PSS coated ITO substrates, which is crucial for successful device operation, resulted from an attractive interaction between the butylamine ligand capped nanocrystals and the PEDOT:PSS electrode. We propose that passivation of the PEDOT:PSS electrode toward unfavourable interfacial dipole formation at the contact with PbS-NC would lead to increased V_{oc} . Furthermore, the FF can be improved by controlled deposition and further ligand removal of PbS-NC, which is expected to increase the shunt resistance and carrier mobility of the nanocrystals, respectively. Therefore, with the above warranted optimizations, an order of magnitude increase of η could be expected from this type of hybrid near-infrared sensitive photovoltaic device.

Acknowledgments

The authors wish to thank the EPSRC for a Portfolio Partnership award and First grant which has facilitated the research conducted in this project and the studentship awarded.

RAH is supported by a Royal Academy of Engineering/EPSRC Research Fellowship.

References

- [1] Kim J Y, Lee K, Coates N E, Moses D, Nguyen T, Dante M and Heeger A J 2007 *Science* **317** 222
- [2] Krebs F C 2009 *Sol. Energy Mater. Sol. Cells* **93** 394–412
- [3] Jørgensen M, Norrman K and Krebs F C 2008 *Sol. Energy Mater. Sol. Cells* **92** 686–714
- [4] Huynh W U, Dittmer J J and Alivisatos A P 2002 *Science* **295** 2425
- [5] Sun B, Snaith H J, Dhoot A S, Westenhoff S and Greenham N C 2005 *J. Appl. Phys.* **97** 14914
- [6] Johnston K W, Pattantyus-Abraham A G, Clifford J P, Myrskog S H, Macneil D D, Levina L and Sargent E H 2008 *Appl. Phys. Lett.* **92** 151115
- [7] McDonald S A, Konstantatos G K, Zhang S, Cyr P W, Klem E J D, Levina L and Sargent E H 2005 *Nat. Mater.* **4** 138
- [8] Dissanayake D M N M, Hatton R A, Lutz T, Giusca C E, Curry R J and Silva S R P 2007 *Appl. Phys. Lett.* **91** 133506
- [9] Hines M A and Scholes G D 2003 *Adv. Mater.* **15** 1844
- [10] Konstantatos G, Howard I, Fischer A, Hoogland S, Clifford J, Klem E, Levina L and Sargent E H 2006 *Nature* **442** 180
- [11] Cademartiri L, Montanari E, Calestani G, Migliori A, Guagliardi A and Ozin G A 2006 *J. Am. Chem. Soc.* **128** 10337
- [12] Brabec C J, Cravino A, Meissner D, Sariciftci N S, Fromherz T, Rispe M T, Shanhez L and Hummelen J C 2001 *Adv. Funct. Mater.* **11** 374
- [13] Khodabakhsh S, Sanderson B M, Nelson J and Jones T S 2006 *Adv. Funct. Mater.* **16** 95
- [14] Mihailetchi V D, Blom P W M, Hummelen J C and Rispe M T 2003 *J. Appl. Phys.* **94** 6849
- [15] Dissanayake D M N M, Lutz T, Curry R J and Silva S R P 2008 *Appl. Phys. Lett.* **93** 043501
- [16] Dissanayake D M N M, Hatton R A, Curry R J and Silva S R P 2007 *Appl. Phys. Lett.* **90** 113505
- [17] Hwang J, Amy F and Kahn A 2006 *Org. Electron.* **7** 387
- [18] Ishii H, Sugiyama K, Ito E and Seki K 1999 *Adv. Mater.* **11** 605
- [19] Hatton R A, Day S R, Chesters M A and Willis M R 2001 *Thin Solid Films* **394** 291–7
- [20] Day S R, Hatton R A, Chesters M A and Willis M R 2002 *Thin Solid Films* **410** 159–66
- [21] Klem E J D, MacNeil D D, Cyr P W, Levina L and Sargent E H 2007 *Appl. Phys. Lett.* **90** 183113
- [22] Koleilat G I, Levina L, Shukla H, Myrskog S H, Hinds S, Pattantyus-Abraham A G and Sargent E H 2008 *ACS Nano* **2** 833
- [23] Peumans P, Yakimov A and Forrest S R 2003 *J. Appl. Phys.* **93** 3693